POLITECNICO DI TORINO
Repository ISTITUZIONALE

Fourier transform based procedure for investigations on the grid frequency signal

Original
Fourier transform based procedure for investigations on the grid frequency signal / Arrigo, F., Merlo, M., Parma, F.. - STAMPA. - 2018-:(2019), pp. 1-6. (2017 IEEE PES Innovative Smart Grid Technologies Conference Europe, ISGT-Europe 2017 ita 2017) [10.1109/ISGTEurope.2017.8260312].

Availability:
This version is available at: 11583/2741172 since: 2019-10-17T19:17:30Z

Publisher:
Institute of Electrical and Electronics Engineers Inc.

Published
DOI:10.1109/ISGTEurope.2017.8260312

Terms of use:

This article is made available under terms and conditions as specified in the corresponding bibliographic description in the repository

Publisher copyright

(Article begins on next page)

10 September 2026

Fourier Transform Based Procedure for Investigations on the Grid Frequency Signal

Francesco Arrigo
Department of Energy
Politecnico di Torino, Turin (Italy)
Email: francesco.arrigo@polito.it

Marco Merlo
Department of Energy
Politecnico di Milano, Milan (Italy)
Email: marco.merlo@polimi.it

Ferdinando Parma
CESI consulting group
Via Rubattino 54, Milan (Italy)
Email: ferdinando.parma@cesi.it

Abstract—the continuous growth of PV and wind sources makes the inertia of the power system decrease and creates larger frequency deviations. Frequency oscillation is a stochastic signal and, consequently, it could be complex to compare the effectiveness of different approaches devoted to manage the problem. In the paper a Fourier transform procedure is proposed in order to define a "standard" frequency oscillation and to set up the dynamic model of the electric grid. The final goal is to numerically simulate a grid depicting a "realistic" transient behavior; such a model results to be the ideal starting point for evaluating the effectiveness of different possible approaches to manage the energy balance problem.

Index Terms—frequency oscillations, Renewable Energy, Stochasticity, Fourier Transform.

I. Introduction

Non dispatchable renewable sources continue to increase in installed capacity in Europe [1] [2]. PV and wind power sources are connected to the electric grid through static power converters and, therefore, they do not contribute to the rotating inertia of the grid [3]. Moreover, power mismatch between Load and Generation will increase due to the stochasticity of renewable primary source (wind velocity and sun radiation), while primary and secondary reserve resources could suffer a decrease as renewable sources are typically not requested to provide frequency regulation [4]. The frequency could divert from the nominal value of 50 Hz for very long periods and with high deviations. This situation could damage the behavior of sensible loads (like electronics components) and saturate power reserve of the grid, endangering the system in case of a generator trip or some other big contingency [5].

To assess possible solutions to this problem, there is a need to simulate a grid depicting a realistic and mathematically defined frequency signal. We have developed a method to replicate the stochastic and deterministic frequency deviations of the grid by reproducing not only the average and standard deviation (SD) of real European data, but also their variability by using discrete Fourier transform (DFT); in particular fast Fourier transform algorithm provided inside the Scipy Stack in Python was adopted. The electric grid simulation is based on a package, named SICRE, developed by CESI Spa and used by Italian TSO Terna Spa [6] [7]. The tool SICRE is able to reproduce electromechanical transients and dynamics phenomena of large power systems.

Analysis of frequency signal was subject to several studies that highlight its importance both for the control of grids and the evaluation of new resources into the grid.

In [8], the nature of frequency signal is studied. The area control error (ACE) of the American electric grid provided by PJM grid operator is analysed using the discrete Fourier transform to highlight the dynamic property of the signal. Distinct peaks in the power spectrum were observed at specific times (5,7.5,10,12,15 and 30 min). Reasons for this phenomenon was found in the market energy operations. The study was performed to create standardized duty-cycle for batteries performing ancillary services into the grid which served in [9] to offer a standard test to evaluate battery system performances.

In [10], the nature of frequency oscillation is studied for Europe. The liberalization of markets led to a worsening of frequency oscillations especially at hour intervals. The causes of the oscillations are: stochastic deviations due to the fast changing of loads (and renewable primary sources) and deterministic frequency deviations which are caused by the changing of production of the Traditional Generation (TG). The TG follows in fact an hour time production schedule built under the market mechanism of the grid. To minimize these deviations, it was suggested to pass to quarterly hour balancing and ancillary service market and limit the TG ramp rate.

In [11] and [12] DFT is used to analyze the frequency signal and divide between its high frequency and low frequency components. Different energy storage technologies were dimensioned to address the specific components of the frequency oscillation. Results depict how batteries are very well suited for very fast oscillations while pumped hydro is more effective in case of slower oscillations.

The paper is organized as follows: in section II, we gather some basic knowledge and parameters relevant to describe the mathematical models adopted to simulate the grid. In section III we address the procedure for the frequency signal creation: in III.A we explain the rationale of using Fourier transform, in III.B, III.C and III.D we go into the details of the procedure and results, and finally in III.E we add some insights and improvement on the

Table I
Topological Elements of the grid

Element	#	Element	#	MW
Power Lines	441	Steam Power Plant	29	2591
Bus Bars	707	Gas Turbine PP	5	273
Two windings transformers	537	Hydroelectric PP	47	2141
Three windings transformers	6	Wind PP	162	1291
Loads	178	Sun PP	60	852

Table II
Primary and Secondary Reserves parameters

Primary	Reserve [MW]	Reserved Band [p.u.]	Droop [p.u.]	Dead Band [mHz]
	250	0.05	0.05	10
Secondary	Reserve [MW]	Units on Service	Propor. Constant [p.u.]	Integral Constant [s]
	307	9	0	120

procedure. Section IV closes the article.

II. Approach proposed and models adopted

As well known, the Swing equation [13] connects the unbalance between produced power and electric power consumed with the frequency deviation Δf of the grid. The goal of the paper is to develop a procedure capable to effectively recreate a realistic frequency signal, this will be obtained perturbing both the generators and the loads in a given grid. For every generation source a stochastic model of oscillation is used to have a realistic profile of power production during the time of simulation. In the procedure proposed, in order to validate the frequency oscillations simulated, a metric based on a discrete Fourier transform has been adopted.

A. Grid static and dynamic main parameters

The grid is based on the open data [14] of the Irish transmission network during winter peak of 2011, when the system was still islanded. In Table I number of main topological elements of our grid and operative capacity in MW are shown.

Static parameters of primary and secondary reserves can be seen in Table II. The models used in simulations are the ones coming from the traditional control loop defined at the EU level [15]: a fixed droop strategy for primary frequency control and a PI control for the secondary control based of the ACE. Different kind of power plants are used to perform the frequency control. To model the different dynamic response of reserves we modelled the power response with a simple answer which is based on two constants T_1 and T_2, the rate limits GRC_{max} and GRC_{min}, which are all dependent on the different technology dynamics. Power response will be of the form:

$$P_m(t) = C_r(1 + (\frac{T_2}{T_1} - 1)exp(-\frac{t}{T_1})) \quad (1)$$

In our grid we modelled steam, hydro and gas turbine time constants, based on numerous references such as [13] [16] [17]. The chosen constants can be seen in II.

B. Stochasticity oscillations models

Stochastic frequency oscillations are correlated to intermittent production from renewable energy sources (PV, wind power, etc.) and to the fluctuation of the loads. The procedure has been developed exploiting the SICRE package. Actually SICRE adopted specific models to realistically reproduce the renewables intermittent production and the stochastic load variations, as detailed in the following.

Wind velocity: wind turbine model (both electromechanical and mechanical part) is described in detail in [7]. Wind power swings will depend on the changing of the wind velocity. Each turbine receives as input a velocity composed by a series of waves of the form:

$$v_{gust}(t) = \frac{A_{rvv}}{2}(1 - \cos(\frac{2\pi t}{T_{rvv}})) \quad (2)$$

where A_{rvv} comes from a random extraction with the following probability distribution function:

$$P(A_{rvv}) = \frac{1}{2\sqrt{\pi}\sigma} e^{-\frac{A_{rvv}}{2\sigma^2}} \quad (3)$$

while T_{rvv} can be written as:

$$T_{rvv} = -\frac{1.48 z_h}{v_{mh}} \ln(1 - (\frac{A_{rvv}}{3\sigma})^2) \quad (4)$$

The unknowns in A_{rvv} and T_{rvv} distribution will then depend on the geometrical and reference velocity parameter of the wind turbine. In particular the inputs of the model are: angle α, radius of the blade r, average height z_m, and the reference height z_r at which corresponds the reference velocity v_{mr}. v_{mr} was decided to be the only parameter to be changed to vary the stochasticity of the component.

Sun Radiation: the extensive description of the PV power plant model can be found in [18]. Also for sun radiation we have an average radiation model which decided the slow changing of G $[W/m^2]$ during the day. A new term ϵ must be added to the average component to model the stochastic passage of clouds. In SICRE, this new term is simulated starting from two random extractions. The first is that of $\dot{\Delta G}$ computed in $Wm^{-2}s^{-1}$ and the second is the time interval of the stochasticity $T_{\Delta G}$. Having this two data we can compute $G_1 = \dot{\Delta G} * T_{\Delta G}$ or the maximum instantaneous offset a time $t + \Delta T_G$. Through a cubic spline this new values are interpolated to give us the instantaneous radiation at time t.

These two distributions are taken from [19] and [20] and corresponds to:

$$f(\dot{\Delta G}) = \alpha e^{-\alpha \dot{\Delta G}} \qquad \alpha = 0.02763 \tag{5}$$

$$f(T) = \frac{\beta}{\alpha^{\beta}} T^{\beta-1} e^{-(T/\alpha)^{\beta}} \qquad \alpha = 3.869 \quad \beta = 1.7109 \tag{6}$$

Load power profiles follow a simple step profile where the new power set point will be randomly extracted from a Gaussian distribution, with a certain settable SD σ around the nominal point. Moreover, we can decide how much time this step will last.

III. Procedure to create the Dynamic Equilibrium

A. Rationale

We can decompose a generic real time discrete series $X = [x_1, x_2, \ldots, x_n]$ with equal time distance between two consecutive data $T_s = \frac{1}{f_s}$ by a sum of sinusoidal terms by applying the DFT to a real discrete series. After some manipulations, we obtain:

$$x(t) = \frac{1}{N} \sum_{k=0}^{N-1} A_k \cos(\phi_k + \frac{k\omega_0 t}{f_s}) \tag{7}$$

f

where n goes from 0 to m and $\omega_o = {}^{2\pi}/_{N}$ is the fundamental frequency with N the number of observations. Therefore, at each harmonic k one can associate an angular frequency $\omega = {}^{k\omega_o}/_{f_s}$ and a corresponding period $T = {}^{2}/_{\omega} = {}^{Nf_s}/_{k} = {}^{T_o}/_{k}$, with T_o the length in seconds of our temporal series. The modules A_k underline the relative importance of the corresponding sinusoid in the global signal. In our specific case, we apply the DFT to the frequency value of the electric grid.

B. Analysis of real data

Real data on the frequency in the Italian electric grid come from experimental measures taken in Politecnico di Milano labs [21] with a sample time of 0.5 seconds over 23 days (measures are relevant to working days in spring and summer 2014).

In figure 1 we can see the DFT of the frequency samples on a 24 h time window, in particular: the graph shows the average of 23 days at our disposal. One can clearly notice the presence of 24 or 12 hours period harmonics, probably caused by the fast increasing and decreasing of the net load in morning and evening hours and the 1 hour peaks which are also driven by market organization.

For the procedure the DFT was applied to every day for any two-hour period which was considered a sufficiently long period to take into account harmonic content and at the same time limiting the computing effort. In figure 2 we can see the average and standard deviation of the module of the harmonics of the 23 days for the time period 8 -10 a.m. (hereinafter the 8.00-10.00 time window will be adopted as a benchmark for the results discussion). As can be seen harmonics are divided into

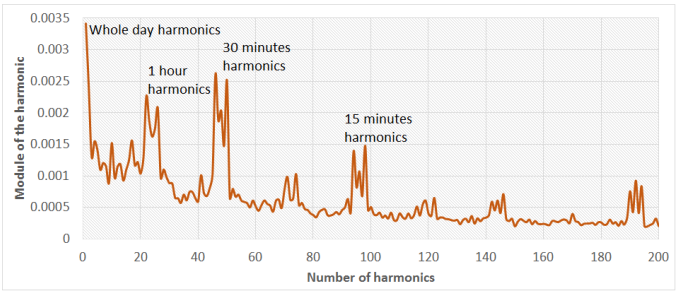

Figure 1. 24 hours Period harmonics for real data

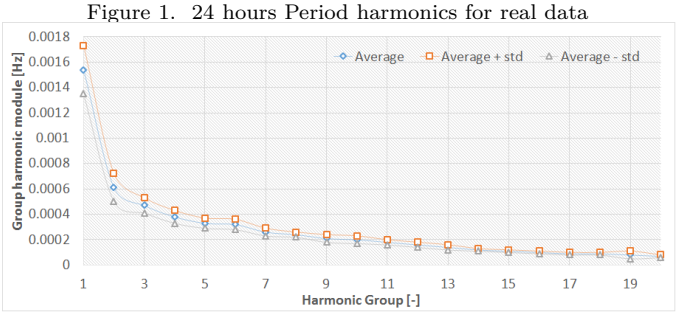

Figure 2. Real Data Module Harmonics Groups

20 harmonics groups: each group is composed by the average value of 20 consecutive harmonics. In such a way similar period harmonics has been grouped simplifying computation and visualization of the spectrum. Of the 7200 available harmonics we have used only 400 modules, which represent 99% of the total value of the spectrum of the signal. Notice how slower harmonics have much higher modulus than faster ones. Such assumptions have been adopted in order to decrease the computational effort of the procedure devoted to simulate the electric grid transients (cfr. frequency oscillation), as detailed in the following.

C. Constructing the dataset of simulations

The next step of the procedure developed is based on the simulation of the electric transient in the Irish grid, evaluating the response of each single component (load, generators, etc.9 With respect to the approach proposed, each component is perturbed with all other elements fixed and the grid frequency oscillation is evaluated. Then in next section different perturbations are simulated simultaneously. The goal is to identify a proper set of perturbations for all the components in order to obtain a frequency oscillation depicting a DFT analysis close the one obtained during the experimental measures. Actually the dataset is composed by the 3 stochastic oscillations presented in section II. In particular parameters evaluated are:

Wind: we choose 5 realistic values for the parameter v_{mr} of each wind turbine going from low wind velocity to very high wind velocity (in figure 3 three example of wind velocity profiles are shown) and then we analyze the corresponding results to obtain the moduli of the grid

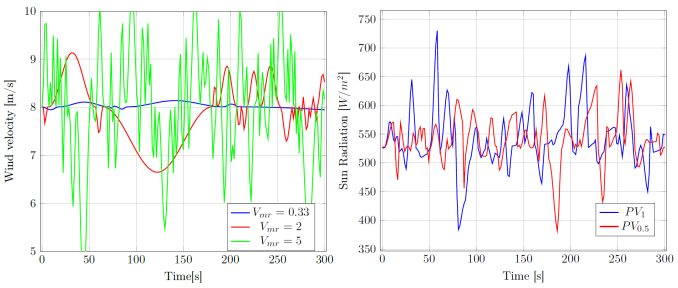

Figure 3. Wind velocity and Sun radiation profiles

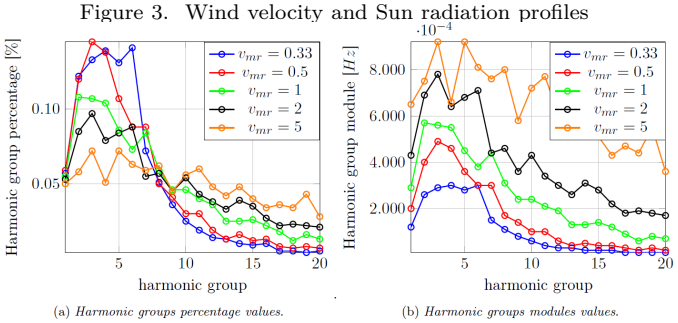

(a) *Harmonic groups percentage values.* (b) *Harmonic groups modules values.*

Figure 4. Wind harmonic Dataset

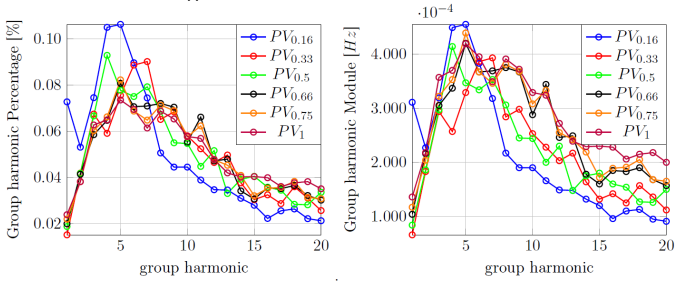

(a) *Group harmonic Percentage Value.* (b) *Group harmonics Modules Value.*

Figure 5. Sun harmonic Dataset

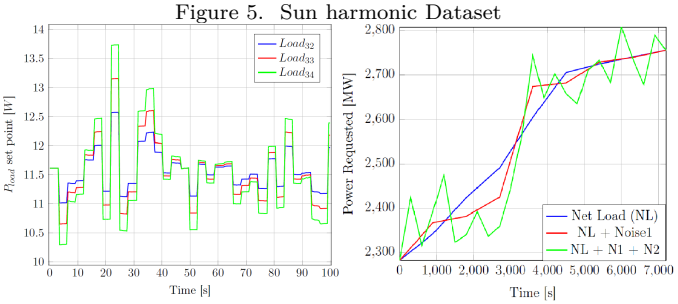

Figure 6. Load and Slow noise power profiles

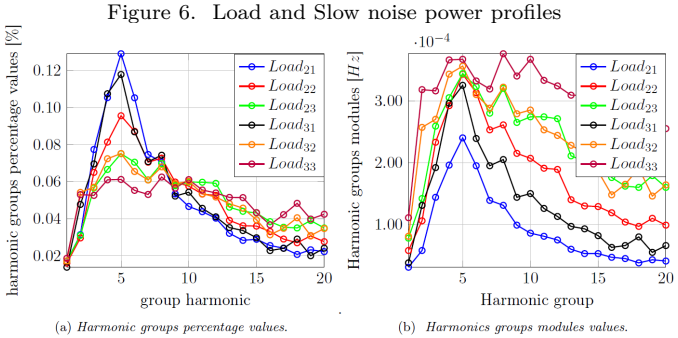

(a) *Harmonic groups percentage values.* (b) *Harmonics groups modules values.*

Figure 7. Load harmonic partial Dataset

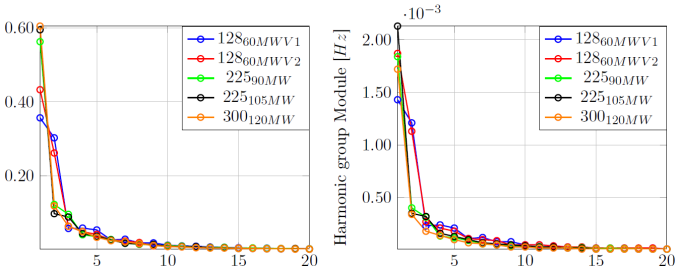

(a) *Harmonic groups percentage values.* (b) *Harmonics groups modules.*

Figure 8. Slow Noise 2 harmonic partial Dataset

frequency harmonics groups. as shown in figure 4. As v_{mr} gets higher results depict a strong impact of wind production on harmonic groups between group 3 to 7.

Sun radiation: as seen from previous section the stochasticity is actually equal in every case (α and β are kept fixed). Examples profiles can be seen in figure 3. We decided to change the amount of Power plants subject to stochasticity as percentage of the maximum capacity present into the grid. Resulting harmonics can be seen in figure 5. The coefficients (from 0 to 1) naming the sun simulations represent the percentages of the PV plants subject to the stochasticity. Most excited frequency harmonic groups are slightly affected by the changing parameter, and correspond from group 4 to 6.

load power profiles: we performed 13 simulations by choosing 4 values for the time step and 4 values for the active power SD σ. The simulations names will be of the form $Load_{xy}$, where x specifies the time in second $t = [1.1, 2.1, 3.1, 4.1]$ of the stochasticity, while y indicates the standard deviation in percentage $\sigma = [1, 2.5, 4, 5.5]$. Example profiles can be seen in figure 6. Resulting harmonics can be seen in figure 7. Harmonics tend to be faster then the other two groups.

Using wind, PV and load noises, we capture only the high frequency part of the frequency signal, which does not permit to replicate satisfactory the harmonic content of real data. There is a need to model also the deterministic oscillations caused by market mechanisms to excite first and second harmonic groups (with periods going from two hour to 180 seconds) [10].

It was chosen to create two new noises using TG as the cause of the unbalance without entering into the details of the electric market models. All generators were kept constant except for the biggest unit which was left to swing and create an instantaneous offset between load and generation.

- The first noise (N_1) accounts for the 15 minutes market schedule organization. Starting from the already known net load, we will extract from a known Gaussian distribution a certain $\Delta P_{OFFSET1}$ every 15 minutes to be summed to the set point of the Generator to create an unbalance into the grid.

- The second noise (N_2) is created to model the fast ramp rates and instantaneous change of TG power set point inside the whole European grid. It was decided to choose a variable $\Delta P_{OFFSET2}$ from a uniform distribution. The time range of $\Delta P_{OFFSET1}$ was chosen to be less than the first noise of 15 minutes.

Only N_2 was actually used in our dataset. It was enough to minimize the difference between real and simulated data. For the name of the simulation, the first number refers to the length in seconds of the power offset extraction, the second to the maximum power offset of the extraction. A vast set of 40 simulations were performed and the time range were taken to be 128, 225 and 300 seconds. In figure 6, two noises example profiles are visualized. In figure 8 N_2 harmonics results for a small group of simulations are shown.

D. Combining the simulations and minimizing the error

Starting from the dataset of single perturbations, we want now to consider them together. If we could predict final global simulations starting from single perturbations values, we could find analytically the combination which give us minimum difference with respect to real data.

As known DFT holds the important property of linearity. Given two time series $x_1[n]$ and $x_2[n]$ with Fourier complex coefficients $\chi_1[k]$ and $\chi_2[k]$ (where the generic $\chi = a + ib$), where k is the harmonic number. Linearity means that if we have a third temporal sequence $x_3[n] = x_1[n] + x_2[n]$ then $\chi_3[k] = \chi_1[k] + \chi_2[k] = \Re(\chi_1) + \Re(\chi_2) + \Im(\chi_1) + \Im(\chi_2)$. In general, for a generic number of signals N we have:

$$|\chi_N[k]| = \sqrt{(\sum_{i=1}^{N} |\chi_i[k]|^2) + (\sum_{\substack{i,j=1 \\ i \neq j}}^{N} \Re(\chi_i)\Re(\chi_j) + \Im(\chi_i)\Im(\chi_j))} \tag{8}$$

In our case, linearity holds only if the frequency signal coming from combining the single simulations can be considered a linear sum of the 4 frequency signals (generically called $f(t)_i$) coming from the 4 different used noises. This means:

$$\Delta freq_{mix} = \Delta freq_{Load} + \Delta freq_{Wind} + \Delta freq_{Sun} + \Delta freq_{SlowNoise2} \tag{9}$$

where the generic $\Delta f_i = f(t)_i - 50[Hz]$, In this case the global simulation harmonic groups are a linear combination of the single perturbation harmonics. This equality is strictly true only for the random stochastic variables of the 4 noises: wind velocity v, sun radiation G, load set point P_{Load} and $\Delta P_{OFFSET2}$. In our case, non linearities can arise in the global simulation, due to saturation and dead-bands inside the components control laws and differential equations. The main non linearity in the simulations is the presence of the dead-band in the primary controller, which affects in a light way the linearity of the results and can be discarded in first approximation.

The error used to compare real and simulated frequency harmonics is:

$$E_i = \begin{cases} |(Ysim_i - (Yreal_i - std_i))|, & \text{if } Ysim_i < (Yreal_i - std_i), \\ (Ysim_i - (Yreal_i + std_i)), & \text{if } Ysim_i > (Yreal_i + std_i), \\ 0, & \text{if } (Yreal_i - std_i) < Ysim_i < (Yreal_i + std_i) \end{cases} \tag{10}$$

$$E_{int} = \frac{\sum_{i=1}^{N_{groups}} E_i}{\sum_{i=1}^{N_{groups}} Yreal_i} \tag{11}$$

where: E_i is the error at the harmonic group i; $Ysim_i$ is the value of the simulated frequency data at the harmonic group i; $Yreal_i$ is the value of the mean of the real frequency data at the harmonic group i; std_i is the value of the standard deviation of the real frequency data at the harmonic i; E_{int} is the integral error for the whole number of harmonics; N_{groups} is the number of harmonic groups. In this case twenty.

A SD is used to guarantee a realistic variability in the results. In figure 9 error computation can be visualized. The goal is to have $E_{int} < 10\%$. 10% is a satisfactory level to validate the procedure and obtain realistic frequency signals. If the error with real data was larger than 10%, we look at the error of the single harmonic groups and we change the intensities of the single perturbations used through the introspection of the dataset previously built trying to excite harmonic groups in a different way.

We applied the above procedure 4 times for our case study. In table III the results are summarized (the pedix number next to the letter W refers to the value of v_{mr} used). The error E_{int} remains under 10% for all the time periods considered. In figure 10 we can see a real frequency signal in red and a signal constructed with our procedure: similarities between the two can be appreciated.

E. Procedure insights and future improvements

By comparing the different noises intensities used, we are now able to understand how much of the total oscillation is correlated to one the noises itself. In particular, neglecting in first approximation the non linearity of the dead-band treated before, we could use the Variance Sum Law for independent variables which holds for the linear combination of N variables:

$$Var_{global} = \sum_{i=1}^{N} Var_i \tag{12}$$

If we divide by Var_{global} and call $Var_{i,pu} = {}^{Var_i}/_{Var_{global}}$ (remember that $Var_i = \sigma_i^2$) we obtain:

Table III
Summarize of chosen simulations

Hours [h]	Name of the perturbation [-]	$\sigma_{Realfreq}$ [Hz]	E_{int} [%]	$\Delta\sigma_{freq}$ [p.u.]	Var_i, pu N_2	PV	Wind	Load
8 -10 a.m	$225_{97.5MW} + PV_{0.5} + W_{0.33} + Load_{21}$	0.0156	5.7	-0.02	0.675	0.20	0.075	0.05
10 - 12 a.m	$300_{105MW} + PV_{0.16} + W_{0.33} + Load_{13}$	0.01427	7.9	0.039	0.665	0.185	0.075	0.075
12 -14 p.m	$225_{105MW} + PV_{0.5} + W_{0.33} + Load_{21}$	0.0175	9.3	-0.067	0.70	0.19	0.07	0.04
14 -16 p.m	$300_{112.5MW} + W_1 + Load_{11}$	0.0146	3.7	-0.02	0.68		0.31	0.01

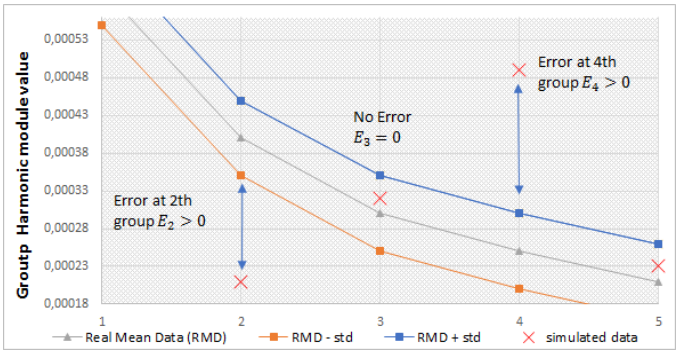

Figure 9. Error calculation Example

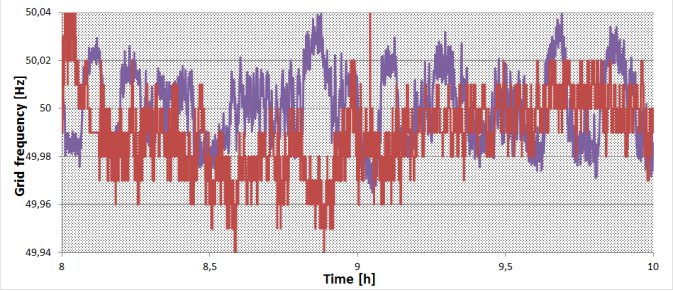

Figure 10. Simulated (red) and real (purple) frequency signal

$$1 = \sum_{i=1}^{N} Var_{i,pu} \tag{13}$$

Even in the real case with the dead-band, equation 13 gives us a good estimate of the various perturbations influence on the global dynamic equilibrium and variance computation for our case study are shown in table III. In the future, we could obtain better results by:

- minimizing the error using harmonic and not harmonic groups. In this way, especially for the first harmonic group, we avoid to mix together harmonic of different periods.
- Taking into account slower harmonics than two hours. In fact, in a two-hour period, the very slow harmonics cause the average of the frequency to be slightly different from 50 Hz.
- Study the non-linearity and take it into account in the perturbation choice.

Both hypothesis can be respected by using the already formed Slow noise N_1. In fact, a 15 minutes noise will be able to hit the first harmonics of a two hour period signal. Besides N_1 will create an unsymmetrical situation inside the two-hour period, able to move the average from 50 Hz. Finally, the procedure can be applied to bigger grids.

IV. Conclusion

In this work, it has been proposed a new approach to study and reconstruct the frequency oscillation by using Fourier Transform valid for any grid configuration. This approach shows good potential. It has been in fact able to highlight the double nature of the frequency oscillation: stochastic, driven by renewable and load sources, and deterministic, driven by market mechanisms. A correct quantification of the two parts can help the system operator taking care in the right way of the frequency instability. The more the stochastic models are realistic the more the final results will be correct. In the future with a realistic frequency signal, our intention is to simulate and evaluate new grid resources like Battery Energy Storage Systems (BESS). In fact BESS performances and useful life when deploying frequency control are deeply correlated to the actual frequency signal present in the grid

Acknowledgment

The authors would like to thank Terna S.p.A. for the possibility to use the SICRE package and prof. Nicola Virgopia for his precious help in revising the work and for encouraging always to reach better results.

References

[1] Iván Pineda Andrew Ho. Wind energy Scenarios for 2030. Tech. rep. Wind Energy Association, 2015.

[2] Frauke Thies Mano'el Rekinger. Global Market Outlook 2015 to 2019 for Solar Power. Tech. rep. Solar Power Europe, 2014.

[3] Entsoe report. Future system inertia. Tech. rep. ENTSOE, 2013.

[4] Zaottini R. Gubernali A. Salvati R. Attachment A15: participation to frequency and load-frequency Regulation. Tech. rep. Terna, 2008.

[5] Entsoe report. Dispersed generation impact on continental Europe Region security. Tech. rep. ENTSOE, 2014.

[6] Entsoe report. Test report on ENTSOE 2nd large-scale CIM interoperability test, Tools Description. Tech. rep. ENTSOE.

[7] G Callegari et al. "Wind power generation impact on the frequency regulation: study on a national scale power system". In: Harmonics and Quality of Power (ICHQP), 2010 14th International Conference on. IEEE. 2010, pp. 1–6.

[8] David Rosewater and Summer Ferreira. "Development of a frequency regulation duty-cycle for standardized energy storage performance testing". In: Journal of Energy Storage 7 (2016), pp. 286–294.

[9] DR Conover et al. Protocol for Uniformly Measuring and Expressing the Performance of Energy Storage Systems. Tech. rep. Sandia National laboratories, 2016.
[10] Response paper. Deterministic frequency deviations root causes and proposals for potential Solutions. Tech. rep. EURELECTRIC - ENTSOE, 2011.
[11] Iman Naziri Moghaddam and Badrul Chowdhury. "Optimal sizing of Hybrid Energy Storage Systems to mitigate wind power fluctuations". In: Power and Energy Society General Meeting (PESGM), 2016. IEEE. 2016, pp. 1–5.
[12] Yuri V Makarov et al. "Sizing energy storage to accommodate high penetration of variable energy resources". In: IEEE Transactions on sustainable Energy 3.1 (2012), pp. 34–40.
[13] Prabha Kundur. Power System Stability and Control. Mc Graw Hill education, 1994.
[14] Eirgrid Website. url: http://www.eirgridgroup.com/.
[15] ENTSO-E. Network Code on Load-Frequency Control and Reserves. 2013.
[16] Göran Andersson. "Modelling and analysis of electric power systems". In: ETH Zurich, september (2008).
[17] Roberto Marconato. Electric power systems. CEI, 2002.
[18] F Parma et al. "A tool to investigate the PV and storage plants effective integration in the European interconnected transmission network". In: Clean Electrical Power (ICCEP), 2013 International Conference on. IEEE. 2013, pp. 254–261.
[19] Teolan Tomson and Gunnar Tamm. "Short-term variability of solar radiation". In: Solar Energy 80.5 (2006), pp. 600–606.
[20] Teolan Tomson. "Fast dynamic processes of solar radiation". In: Solar Energy 84.2 (2010), pp. 318–323.
[21] S Nassuato et al. "Distributed Storage for the Provision of Ancillary Services to the Main Grid: Project PRESTO". In: Energy Procedia 99 (2016), pp. 182–193.